Heat Transfer Measurements Using Thin Film Gauges and Infrared Thermography on a Film Cooled Transonic Vane

Colin J. Reagle

Thesis submitted to the faculty of Virginia Polytechnic Institute and State University in partial fulfillment of the requirements for the degree of

Master's of Science
in
Mechanical Engineering

Dr. Wing Ng, Co-Chair
Dr. Srinath Ekkad, Co-Chair
Dr. Thomas Diller

May 4, 2009
Blacksburg, VA

Keywords: Heat Transfer, Film Cooling, Turbine, Vane, Transonic, Cascade, Infrared

Heat Transfer Measurements Using Thin Film Gauges and Infrared Thermography on a Film Cooled Transonic Vane

ABSTRACT

This work presents a comparison of thin film gauge (TFG) and infrared (IR) thermography measurement techniques to simultaneously determine heat transfer coefficient and film cooling effectiveness. The first comparison was with an uncooled vane where heat transfer coefficient was measured at M_{ex}=0.77 and Tu=16%. Relatively good agreement was found between the results of the two methods and the effect of recovery temperature and data reduction time was analyzed. Improvements were made to the experimental set up for the next comparison, a showerhead film cooled vane. This geometry was tested at BR=0, 2.0, M_{ex}=0.76 and Tu=16%. The TFG and IR results did not compare well for heat transfer coefficient or film cooling effectiveness. The effects of measured and calculated recovery temperature were analyzed as well as the respective data reduction methods, though the analysis could not account for the effectiveness trend seen on the suction surface. Finally, a vane with showerhead and shaped film cooling holes were presented at BR=0, 1.7, 2.0, 2.8, M_{ex}=0.85, and Tu=13% to assess a new film cooling geometry measured with the IR technique. Similarities on the suction surface trend between the different film cooled geometries tested with IR indicate a flaw in the experiment that will require further analysis, changes and testing to complete the comparison with TFG.

ACKNOWLEDGEMENTS

First, I would like to express my gratitude to Solar Turbines and Drs. Moon and Zhang for sponsoring my work these past two years. I hope I have been able to return the investment to their company that they've made in me and my degree.

I would like to express my sincere gratitude to my advisor Dr. Wing Ng. Through his leadership, experience, and trust I have learned more as a scholar than I ever expected when I applied to graduate school. I would also like to thank Dr. Srinath Ekkad for his hours of discussion and advice. My understanding of heat transfer and gas turbine hardware has flourished under his guidance. Thanks are also in order for Dr. Thomas Diller for his independent review of my research and thesis which undoubtedly improved the quality of my work.

This work has been helped along by many people in the Department of Mechanical Engineering at Virginia Tech. I would like to thank Bill Songer, Johnny Cox, and James Dowdy from the shop for their machining expertise, rush jobs, and good humor, Ben Poe and Jamie Archual in the computer department for troubleshooting, advice, and quirky jokes and emails, Melissa Williams, Kathy Hill, and all the ladies in the main office for answering countless questions and requests.

To my research colleagues, I'd first like to thank Shakeel Nasir and Trey Bolchoz. They were great examples of how graduate students should be and much of my attitude and outlook was modeled after their example. To Drew, Santosh, Kapil, and Song I would like to say thank you for your dedication and help completing our research. You have made coming to campus everyday a joy and from our discussions academic and otherwise, I feel like I've become a more worldly and knowledgeable human being.

I would especially like to thank my friends from Virginia Tech and Centreville, VA for providing the necessary rest, relaxation, and general good times to keep me from going crazy these past six years. For the days and nights in Blacksburg, the spring breaks, the soccer tournaments and trips, the weekends and weeks at home, it's helped keep everything balanced in my life. I wouldn't feel right naming names because I'd surely leave someone out, but you know who you are. Thank you.

Most importantly I'd like to thank my parents, Bill and Paulette, and my sister Jessica. Without their love and support I'd never be where I'm at today. Words really aren't enough to thank them. Miss Ella I won't forget you either, even though you'll never be able to read this.

TABLE OF CONTENTS

LIST OF FIGURES AND TABLES

INTRODUCTION

Since the first gas turbine commercial application, engine designers have been striving for the same goal, to output more power for a longer time. One way to increase power output from the Brayton cycle is to increase turbine inlet temperature. Temperatures have already far surpassed the limit of conventional metals so more efficient ways of cooling engine components must be developed in order to raise inlet temperatures. Film cooling is a widely used technique in which relatively cool air is bled from the compressor section of the engine and injected through discrete holes in the surface of turbine components providing a protective film. This technique reduces thermal fatigue, hence improving the reliability and longevity of gas turbine engines. Research in gas turbine heat transfer and cooling has been in progress since the 1960's but more recent advances in film cooling technology have been in the application of shaped holes. Shaped holes can provide better coolant coverage than cylindrical holes, but there are many variables that influence their effectiveness. Since coolant does not contribute to the power cycle of a gas turbine engine, a balance must be found between output and reliability. Even with the advances in computer technology, computation methods cannot accurately assess all variables in this complex three temperature convection problem. Experiments are still required to validate and quantify film cooling performance.

The main objective in this experiment is the adaptation and validation of infrared thermography in a transonic cascade facility. Previous heat transfer coefficient and effectiveness results in the Virginia Tech transonic cascade have been measured using thin film gauges along the midspan of the vane. Transient surface temperature is measured at identical flow conditions in an identical facility only using different sensors. An uncooled and a showerhead film cooled nozzle guide vane are used for comparison between TFG and IR. A second film cooling geometry with two rows of fan shaped holes and five rows of showerhead film cooling holes is used to compare IR measurements with a second film cooled vane at transonic conditions.

PAST STUDIES

Film cooling has been a widely researched topic. Many different works from the gas turbine community were studied before, during and after the experiments discussed in this thesis. A summary of these works is presented here.

Many different measurement techniques are available to characterize turbine vane heat transfer including thermocouple based techniques, mass-transfer analogy techniques, optical techniques, each offering its own benefits and drawbacks. Han *et al.* [1] have compiled a list of different methods and the operating theory behind them for both transient and steady state testing. Thin film gauges provide fast response, low resolution temperature measurements over real airfoils after extensive instrumentation. Infrared thermography is a non-intrusive technique with high spatial resolution which can be used in high temperature environments with sufficient optical access.

A recent summary by Bogard and Thole [2] of film cooling research has cited mass flux ratio, momentum flux ratio, freestream turbulence, hole geometry, and surface curvature as significant factors in film cooling performance. Bunker [3] assembled a through review of shaped hole film cooling technology and the effects of blowing ratio, injection angle, and freestream turbulence and their effects on heat transfer coefficient and film effectiveness.

Abuaf *et al.* [4] determined heat transfer coefficient and effectiveness simultaneously in a transient cascade at high freestream turbulence. Significant heat transfer coefficient augmentation due to combined showerhead and suction surface film cooling injection was observed on the suction surface compared to the uncooled vane.

Guo *et al.* [5] applied thin film gages to measure heat transfer coefficient and effectiveness over a heavily film cooled nozzle guide vane at high freestream turbulence. Higher heat transfer coefficient levels were observed directly downstream of coolant injection, though further downstream the levels often dropped below those of the uncooled vane. Cylindrical holes were shown to increase heat transfer coefficient levels above those of fan shaped holes due to higher momentum jets disturbing the boundary layer.

Reiss and Boelcs [6] studied the effects of boundary layer state and Reynolds number on airfoil film cooling performance using liquid crystals. A single cylindrical

injection location on the suction surface was tested. For the uncooled case, cooling holes locally disturbed the laminar boundary layer and caused increased heat transfer levels downstream of the holes. At the nominal flow condition, heat transfer was only marginally affected by blowing ratio for turbulent and laminar boundary layer. Turbulent boundary layers were shown to dilute the coolant and decrease effectiveness downstream of injection compared to laminar boundary layer.

Zhang and Moon [7] used pressure sensitive paint to experimentally investigated the effect of wall thickness on film cooling effectiveness using the same vane geometry as presented in this paper. Effectiveness distributions were presented for the suction side at various blowing ratio. They concluded that showerhead film cooling effectiveness increases with blowing ratio in general. They also concluded that film effectiveness for showerhead combined with suction side shaped injection increases with blowing ratio but jet lift off was observed at higher blowing ratios.

Ekkad *et. al.* [8] developed an infrared thermography technique which measures transient surface temperatures to simultaneously determine heat transfer coefficient and film cooling effectiveness. This method has many advantages over its liquid crystal counterpart in that expensive surface preparation is eliminated, it reduces uncertainty associated with running two different tests, the temperature range is not limited by the operating point of the crystals and it accounts for non-uniform initial temperatures. Results are presented for a leading edge model at different blowing ratios. This technique is the basis for the IR measurements presented in this experiment.

NOMENCLATURE

A	area
BR	blowing ratio
C	vane true chord
C_d	discharge coefficient
C_p	constant pressure specific heat capacity
d	cooling hole diameter
DR	density ratio

h	heat transfer coefficient
IR	infrared
K	acceleration parameter
k	thermal conductivity
M	Mach number
$\dot{m}$	mass flow rate
P	vane pitch
p	cooling hole pitch
Pr	Prandtl number
PS	pressure side
$q"$	heat flux
R	gas constant
r	recovery factor
SS	suction side
T	temperature
TFG	thin film gauge
Tu	streamwise freestream turbulence intensity
U	local velocity
X	vane surface distance from stagnation point
y	surface depth

Greek

γ	compound angle (streamwise) or ratio of specific heats
α	injection angle (spanwise) or thermal diffusivity
η	adiabatic film cooling effectiveness
ρ	local density of air

Subscripts

0	no film cooling
∞	freestream
aw, w	adiabatic wall, wall

c	coolant
ex	exit
o	stagnation
r	recovery
s	surface
t	total

EXPERIMENTAL SETUP

Virginia Tech Transonic Cascade

The Virginia Tech Transonic Cascade facility shown in Figure 1 is a blow down facility capable of sustaining test section inlet pressure for up to 25 seconds. Air is supplied from high pressure tanks that are charged up to 160 psig (1100 kPa) prior to discharge. A control valve upstream of the test section regulates flow from the air tanks. Between the control valve and the test section, a heater and a passive heat exchanger warm the air to approximately 240°F (115°C) at tunnel start. After the air exits the heat exchanger it passes through a contraction, then through a passive turbulence generation grid before entering the test section. This facility has been used by Smith *et al.* [9], Popp *et al.* [10], Nix *et al.* [11], Carullo *et al.* [12], Nasir *et al.* [13, 14], and Bolchoz *et al.* [15] to separately measure both vane and blade heat transfer.

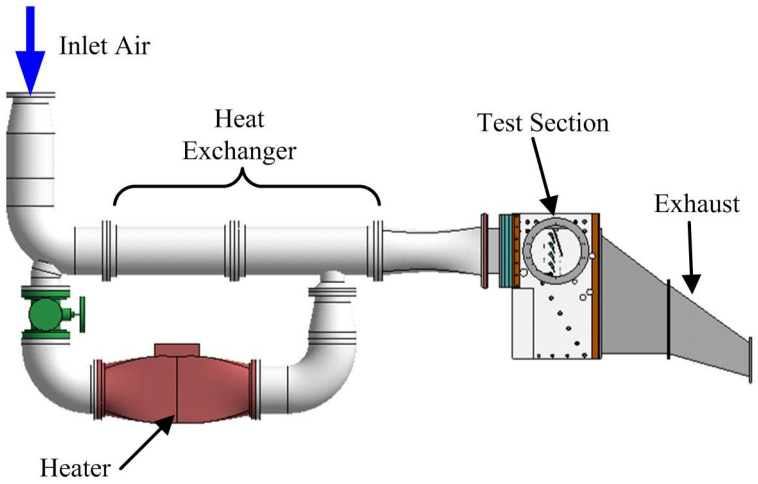

Figure 1. Virginia Tech Transonic Cascade

The vane cascade consists of four full vanes and two half vanes for a total of four full passages and one partial. A tailboard was placed at the trailing edge of the topmost half vane to ensure periodicity as shown by Nasir *et al.* [13]. Inlet pressures are measured by a Pitot-static probe while inlet temperature is measured by a T-Type, air thermocouple near the inlet of the test section. All heat transfer measurements were made on the center vane.

Vane Geometry

Results from three different vane geometries are studied in this work. All vanes are based on the same profile taken from an engine representative, first stage turbine vane. The vane was scaled 1.5 times to obtain the proper Reynolds number. All heat transfer and film cooling vanes were machined out of Macor, a machinable ceramic material with desirable thermal properties for 1-D, semi-infinite heat transfer assumption. The first set of measurements was made on a solid, uncooled vane described in Table 1.

Table 1. Uncooled Vane Geometry

True Chord, *C*	3.59 in. (91.2 mm)
Axial Chord	1.97 in. (50.0 mm)
Pitch, *P*	3.27 in. (83.0 mm)
Span	6.00 in. (152.4 mm)
Inlet and Exit Angle	0° and 73.5°

The second set of measurements was made on a vane with the same physical dimensions as the uncooled vane, with the addition of a showerhead film cooling scheme. The scheme consisted of 83 cylindrical holes in five rows centered on the leading edge. The geometry is shown below in Figure 2 and 3 and tabulated in Table 2.

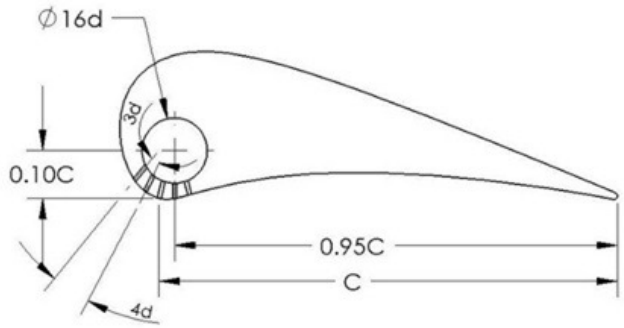

Figure 2. Showerhead Film Cooled Vane.

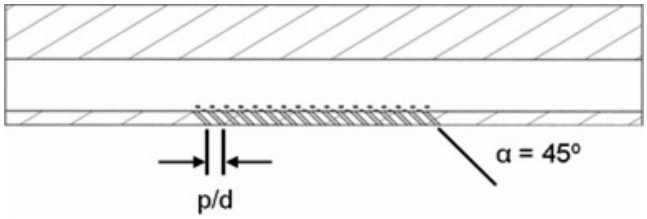

Figure 3. Sectioned View of Stagnation Row of Holes

Table 2. Showerhead Film Cooling Geometry

Cooling Hole Diameter	*d*	0.031 in. (0.787mm)
Cooling Hole Spacing	*p/d*	4.35
Injection Angle (spanwise)	α	45°
Compound Angle (streamwise)	γ	90°
Cooled Span		2.33 in. (59.2 mm)

The third set of measurements were made on a vane with a showerhead cooling scheme identical to the one described in Figure 2, Figure 3, and Table 2 with the addition of two rows of shaped film cooling holes, 19 per row. The common plenum diameter was enlarged from 16d to 20d to supply the additional two rows. Figure 4 shows the shaped hole vane geometry with injection locations. The pressure and suction side holes

are called 10 degree layback holes because they diffuse symmetrically 10 degrees in the spanwise direction, and asymmetrically 10 degrees in the streamwise direction. Details of the diffuser shape are described in Figure 5 and tabulated in Table 3.

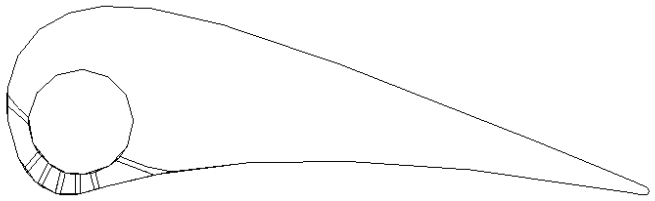

Figure 4. Shaped Hole Vane Geometry

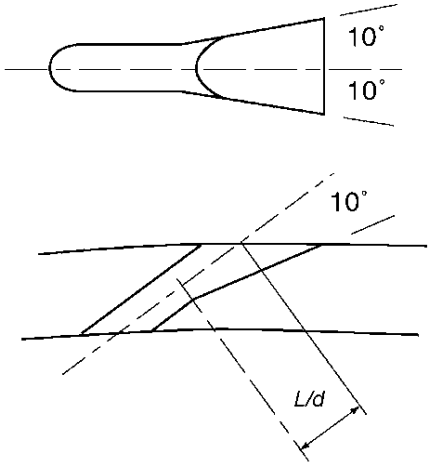

Figure 5. 10 Degree Layback Hole.

Table 3. Shaped Hole Geometry

Metering Section Diameter	*d*	0.031 in. (0.787mm)
Cooling Hole Spacing	*p/d*	3.5
Shaped Hole Length	*L/d*	2.5
Injection Angle (spanwise)	α	90°
Suction Side Compound Angle	γ	50°
Pressure Side Compound Angle	γ	35°

Film Cooling Supply

Coolant for the film cooled vanes was filtered, dried, then stored at 120psig in a separate air tank. The coolant supply was controlled by a valve which was set before each run. The film cooling air passes through an orifice flow meter then through a heat exchanger which was adjusted so the coolant temperature matched the initial temperature of the vane prior to every run. The coolant supply was set to provide a specific coolant to mainstream mass flux ratio, or blowing ratio, defined as:

$$BR = \frac{\rho_c U_c}{\rho_\infty U_\infty} \tag{1}$$

For the showerhead cooled vane the blowing ratio was calculated by measuring the total mass flow of the coolant and assuming it was evenly distributed through the five rows of showerhead holes. This gave an approximate local coolant velocity which could be used for the entire region to calculate blowing ratio. Freestream density and velocity were determined by a Pitot-static probe and a T-Type thermocouple.

For the shaped hole vane, blowing ratio calculations were much more complicated since a single plenum was supplying coolant to three distinct surface locations. To determine how much coolant went to each row, the discharge coefficients:

$$C_D = \frac{\dot{m}_{actual}}{\dot{m}_{ideal}} \tag{2}$$

for each row were used. The discharge coefficient accounted for hole geometry and local pressure variations. Gritsch [16] calculated the ideal mass flow assuming isentropic, 1-D expansion using the equation:

$$m_{c,ideal} = A_c P_{t,c} \left(\frac{P_{\infty,s}}{P_{t,c}} \right)^{\frac{\gamma+1}{2\gamma}} \sqrt{\frac{2\gamma}{(\gamma-1)RT_{t,c}} \left[\left(\frac{P_{t,c}}{P_{\infty,s}} \right)^{\frac{\gamma-1}{\gamma}} - 1 \right]} \tag{3}$$

where all the coolant properties are known and the surface pressure at each injection location was measured using a surface pressure tap on an adjacent vane in the cascade. With the discharge coefficient for a specific pressure ratio and the calculated ideal flow rate, the actual mass flow could be calculated and the blowing ratio determined.

Another film cooling variable of interest is coolant to mainstream density ratio which is defined as:

$$DR = \frac{\rho_C}{\rho_\infty} \tag{4}$$

Typical engine density ratios are approximately 2, however, due to the difficulties associated with achieving such high levels in an experimental facility, density ratio was measured but not matched. Bogard and Thole [2] have suggested that the effects of density ratio are secondary to matching blowing ratio, momentum flux ratio, or velocity ratio to engine conditions. Typical levels in this experiment were between 1.3 and 1.4.

Infrared Measurements

Previous heat transfer and film cooling effectiveness measurements [12,13,14,15] in this facility have been made using thin film gauges. This section describes the modifications necessary to make infrared measurements in a high speed cascade. In TFG experiments, Lexan or aluminum test section windows were used to extract pressure and temperature measurements from the instrumented vanes while maintaining pressure in the cascade. To make temperature measurements using an infrared camera, an additional IR transparent window needed to be added with line of sight to the vane surface [1]. Due to the large forces seen in a transonic facility, the window also needed to be structurally sound. A 4in diameter Zinc Selenide window was used to satisfy both of these design constraints. To view the locations of interest on the vane, 3 window locations were used to measure surface temperatures. They are shown in Figure 6 below.

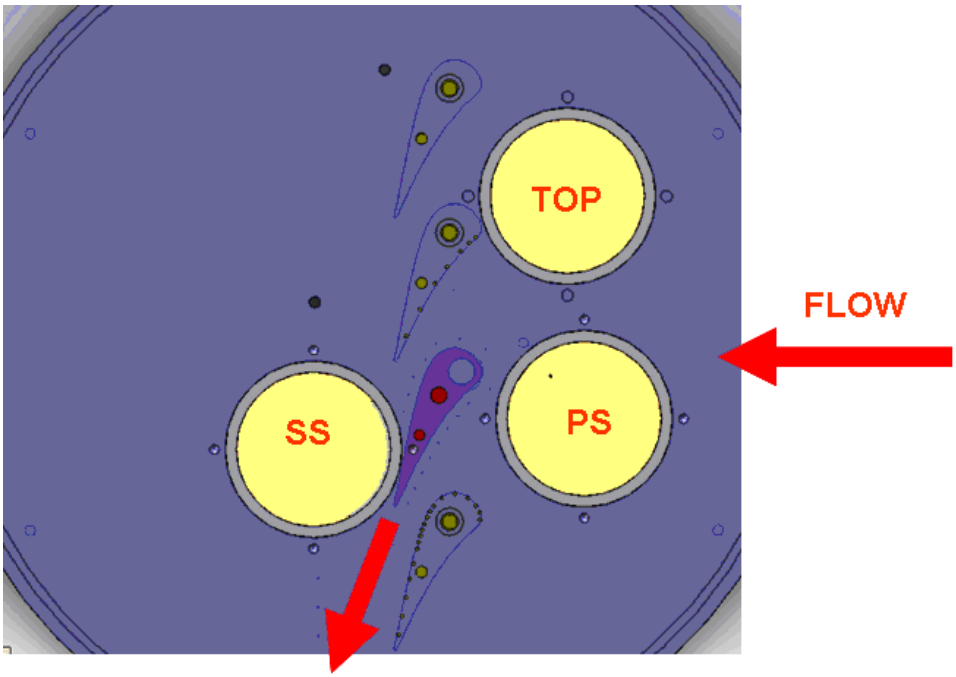

Figure 6. IR Window Locations.

Ideally, the IR window would have a transmission of 100% and the vane would act as a blackbody for radiation. The addition of anit-reflective coating on the Zinc Selenide window increased the infrared transmission to 99%. To increase the emissivity and reduce the reflected radiation, the vane was painted with flat black paint which increases the emissivity of the object to approximately 95%. An example view of the film cooled vane from the PS window is shown below in Figure 7. Most of the heat transfer coefficient plots and film cooling effectiveness plots are at an angle to the vane surface and plotted in color from blue to red according to value, which can be somewhat disorienting. A grid has been painted on the surface of the vane to help in locating vane midspan and also orient the IR images for the reader. Surface thermocouples have also been mounted near the endwall under a 1" thick piece of Kapton tape which will be discussed further in the Data Reduction section.

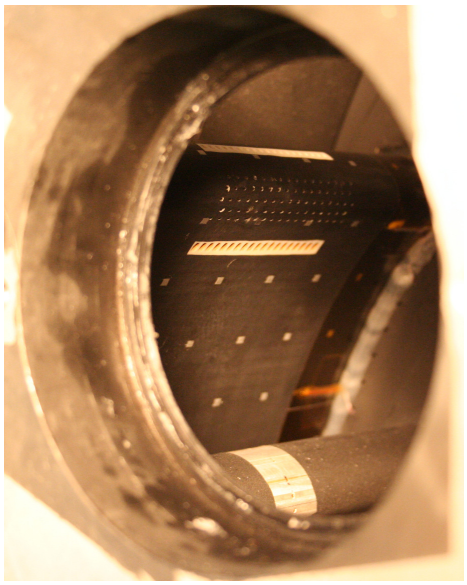

Figure 7. Example view of Shaped Hole Vane from PS window location

DATA REDUCTION

Both techniques, IR and TFG, use a low thermal conductivity material and reduce data over a short duration, so the 1-D, semi-infinite heat flux assumption can be used. There is also significant cool down times in between runs so the vane is at a uniform initial temperature. In film cooling measurements, the coolant temperature is adjusted to match the initial temperature of the vane to minimize internal conduction.

Despite the similarities, there are two major challenges with reducing the IR data. For thin film gauges, a sheet of approximately 25 gauges is wrapped around the scaled vane to measure midspan surface temperature. The infrared camera, at 640x480 resolution, can measure 307,200 surface temperatures simultaneously. The major advantage of the IR camera is seeing temperature measurements and spanwise variation instead of midspan voltage output. The downside is that, while the TFGs stay fixed to a surface location, the camera is moved outside of the cascade and takes temperature measurements regardless of where the vane surface is in the image frame. The difference in measurement technique between TFGs and infrared thermography caused us to examine using a different data reduction method as well. The TFG and IR data reduction techniques are split up into separate sections for both the uncooled and film cooled versions.

UNCOOLED VANE COMPARISION

Thin Film Gauge Data Reduction

The basic equation governing convective heat transfer into a surface is defined as:

$$-k\left.\frac{\partial T}{\partial y}\right|_{y=0} = q'' = h(T_{aw} - T_w) \tag{5}$$

where y is the surface depth, T_w is the wall temperature, and T_{aw} is the adiabatic wall temperature, the driving temperature for heat transfer. For uncooled cases, the thin film gauge technique assumes that, T_{aw} is equivalent to T_r, the recovery temperature. Recovery temperature is dependent on the speed of the flow and can be approximated using the equation:

$$T_r = T_{o,\infty}\left(\frac{1 + r\frac{\gamma - 1}{2}M^2}{1 + \frac{\gamma - 1}{2}M^2}\right) \tag{6}$$

where $T_{0,\infty}$ is the inlet total temperature in Kelvin, M is the local surface Mach number, and r is the recovery factor ($\mathrm{Pr}^{1/3} = 0.892$).

Using the TFG method, a 2 layer finite difference code calculates heat flux, *q"*, from the temperature history of the gauge and the properties of the TFG and Macor substrate. An example temperature history and *q"* history is presented in Figure 8. Recovery temperature is calculated from equation 6, and the only unknown left in equation 5 is h, which is calculated at every sample and averaged for 0.25s once the tunnel reaches the objective Mach number.

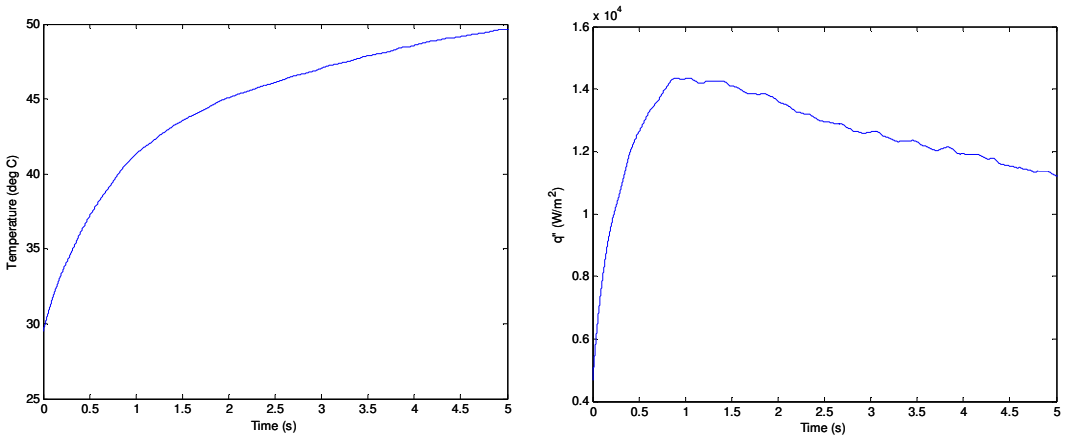

Figure 8. Example Temperature Trace and Heat Flux Calculation using code

Infrared Data Reduction Matlab Method

To reduce the infrared data, it would be ideal if the data could be processed based on temperature images alone, without knowledge of surface location. To do so would require an equation that was a function of only *h* and our known values. Carslaw and Jaeger [17] derived such an equation by first introducing the general form of the conduction equation:

$$k\frac{\partial^2 T}{\partial y^2} = \rho C_p \frac{\partial T}{\partial t} \tag{7}$$

where ρ and C_p are the density and specific heat of the material respectively. The boundary and initial conditions are defined as:

$$T_{t=0} = T_i \tag{8}$$

$$T_{y=\infty} = T_i \tag{9}$$

which complete the differential equation set. To finish the derivation, equation 5 is combined with equation 7 and the initial, equation 8, and boundary, equation 9, conditions are applied to produce a solution of the form:

$$\frac{T_w - T_i}{T_\infty - T_i} = 1 - \exp\left(\frac{h^2 \alpha t}{k^2}\right) erfc\left(\frac{h\sqrt{\alpha t}}{k}\right) \tag{10}$$

where h is the only unknown. This solution makes the simplification that T_{aw} is equivalent to T_∞ in equation 5. To solve for h, the measured wall temperature history is curve fit to the solution derived above using a Matlab program and the fminsearch function to minimize error in the curve fit. A sample curve fit is presented in Figure 9. The data reduction window for this method is 0-5s. Surface location is not considered in this data reduction method because recovery temperature is not used.

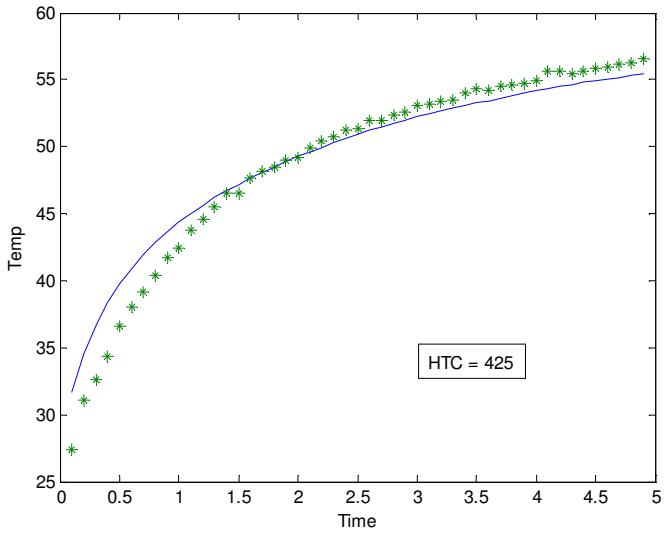

Figure 9. Example curve fit of Uncooled Vane IR Data

Post Processing

One of the challenges taken on during this comparison was converting a set of 2D IR images of a 3D vane into a 1D line plot to compare with the TFGs. The TFGs were permanently mounted on the vane and always measured temperature at the same surface location during every run. The IR camera is positioned outside the tunnel and moved from one window to the next during testing. To compare with midspan data from the

TFGs there must be an accurate way to find midspan in the IR image and extract the desired data.

This was accomplished using the actual vane profile points that were provided by the project sponsor, Solar Turbines. There are a number of reference points that can be found in the IR image due to different surface and thermal properties, such as a 1" thick piece of Kapton tape and the metallic grid that was painted onto the surface. Starting with an easy to identify reference point, such as the leading edge and Kapton tape junction, the profile points are mapped onto the image at this reference. An offset is then applied to create a second curve at midspan. Both curves are then scaled to match the profile points with the grid points painted on the surface. Due to test section geometry, the camera cannot view the vane straight-on and a horizontal angle adjustment must be made. The angle is adjusted so the first curve matches the edge of the Kapton tape using a transformation. Finally, a similar vertical angle adjustment is made to correct for the height of the camera relative to the vane. The profile mapping is iterated until the curves match all of the reference points on the vane. An example of the completed process is shown in Figure 10. After this process, specific surface locations are known by pixel location and it is possible to extract values from the 640x480 matrix using these locations.

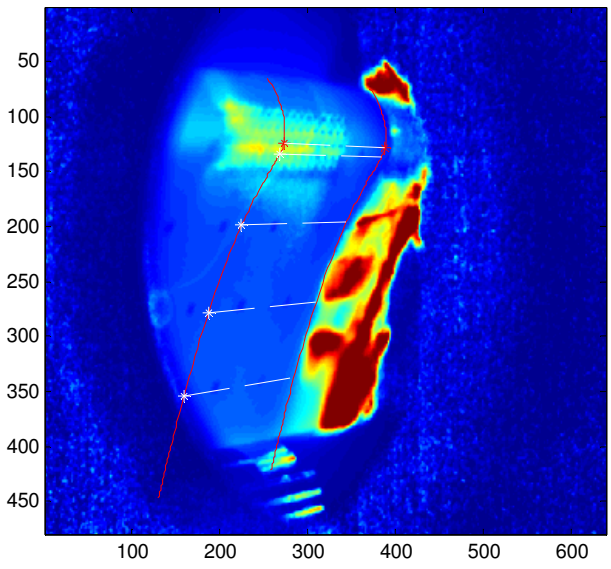

Figure 10. Example of Vane post processing

Results

The uncooled vane comparison between thin film gauge and infrared measurement results is presented below in Figure 11. Only one exit Mach number of 0.77 was tested at an inlet turbulence intensity of 16%. This is to match and compare with the results of Nasir *et al.* [12]. There is reasonably good comparison between the trends of the two techniques. Both methods predict high levels of heat transfer coefficient at the leading edge which decrease by approximately 50% further downstream on each surface. On the suction surface, heat transfer coefficient rapidly increases downstream of X/C=0.5 caused by laminar to turbulent boundary layer transition. Two areas don't compare well between the IR and TFG data sets, specifically the area of 0.2<X/C<0.4 and the trailing edge regions.

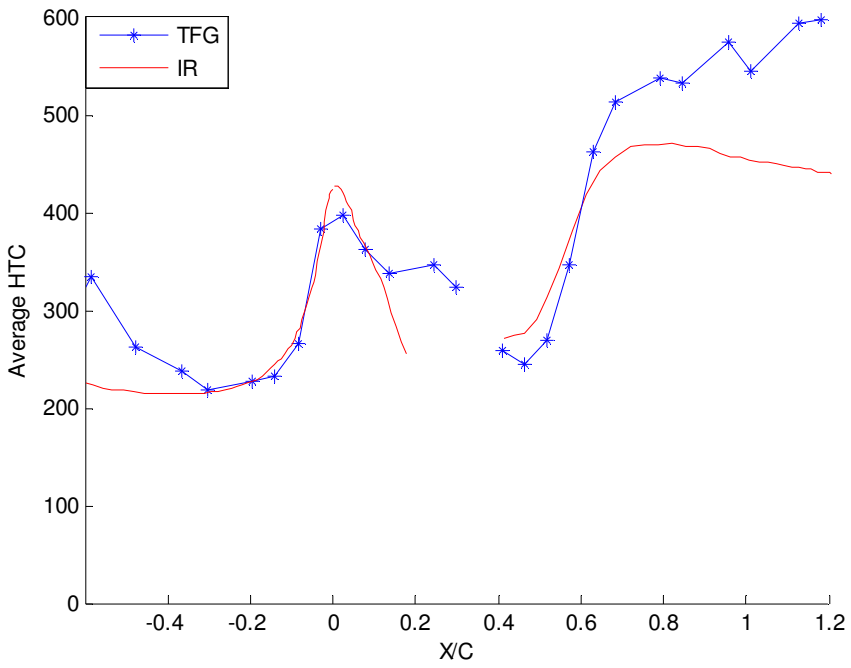

Figure 11. Uncooled Results at M_{ex} = 0.77, Tu = 16%

Analysis

The first region, 0.2<X/C<0.4, is due to only having PS and SS windows during the uncooled testing. It was discovered during post processing of the uncooled data that this region could not be viewed resulting in the third, TOP, window being added for subsequent testing. Details can be seen in Figure 6. The second region, the trailing edge, requires more analysis.

In theory, both techniques measure surface temperature in an identical facility and should produce identical results. The theory behind the reduction is also identical in that 1-D semi-infinite heat flux is assumed for a transient mainstream temperature. The discrepancies in the trailing edge data may be accounted for by the differences in how the raw data is reduced. The first difference is that the IR data reduction used in Figure 11 does not account for the recovery temperature effect caused by high surface Mach numbers due to challenges identifying surface location in the image. The variable T_d is defined as:

$$T_d = T_{0,\infty} - T_r \tag{11}$$

for future discussion. Figure 12 plots the TFG data with and without the effect of recovery temperature. Recovery temperature does not have a noticeable effect on the pressure surface, however it may account for some of the discrepancies on the suction surface trailing edge region where high surface Mach number effectively increases heat transfer coefficient by decreasing T_{aw}. Incorporating recovery temperature into the IR data would also raise the heat transfer coefficient in this region and the results would compare more favorably.

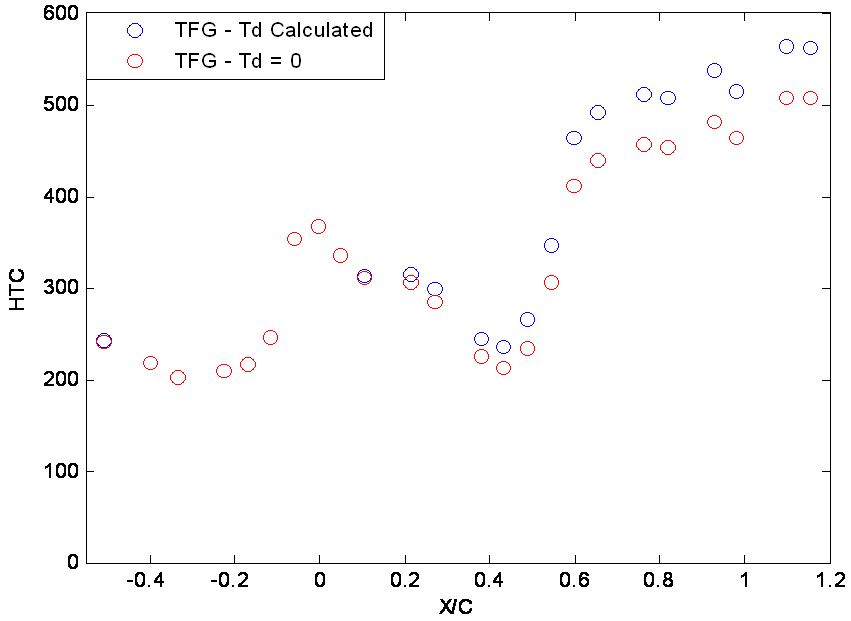

Figure 12. Effect of Recovery Temperature on Uncooled TFG data.

The two techniques also use different data reduction times. The IR technique uses approximately 5 seconds worth of data including the tunnel ramp up while the TFG technique uses 0.25s worth of data right after the tunnel ramp up occurs as shown in Figure 13. The red, green, and black double lines represent different possible data reduction windows during the tunnel run. Most of the gauge locations exhibit steady *h* over time, however, some of the gauges near the trailing edge region have decreasing *h* during the run. Two gauges *h* histories are plotted in Figure 14 for a single run. This would help further explain the trailing edge discrepancies. If the TFG *h* data was averaged over a longer period, up to 5s as the IR data was, it would decrease the values at these locations and the results would compare better.

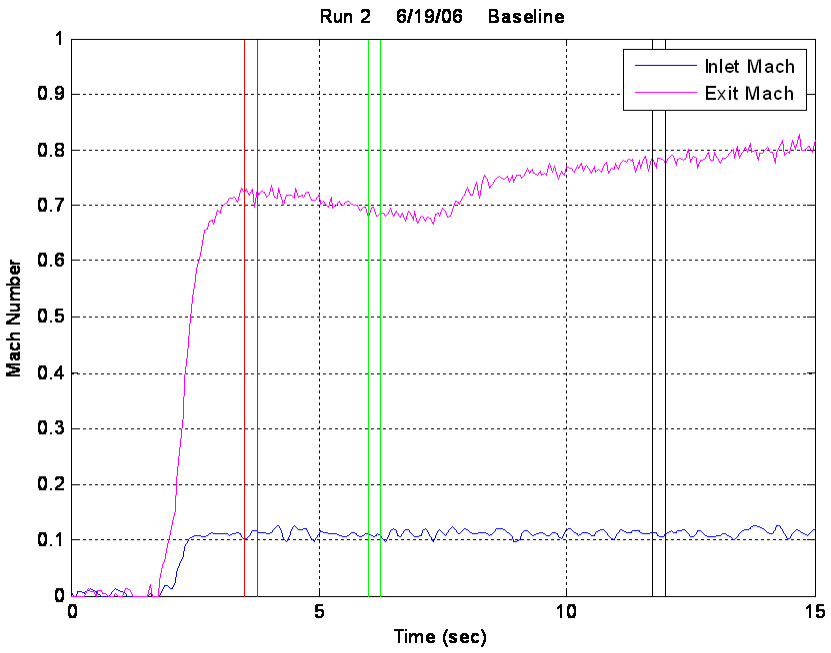

Figure 13. Sample tunnel response from uncooled TFG testing

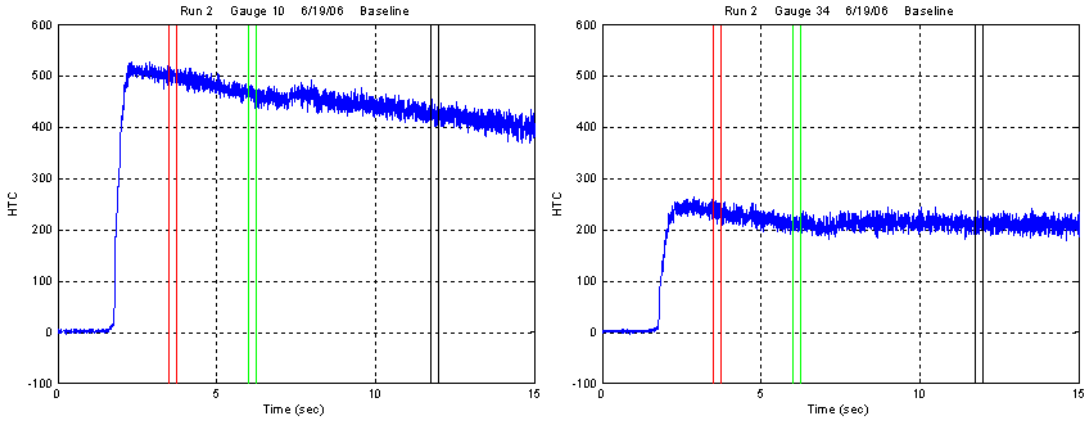

Figure 14. Sample Gauge output for X/C = 0.817 and -0.506 respectively.

Finally, the TFG technique uses a two layer, finite difference code to calculate heat flux at each sample time while the IR technique does not directly calculate heat flux, but incorporates it into the wall temperature solution, equation 10. This effect is also incorporated into the TFG film cooling data reduction and will be discussed further in the Data Reduction Analysis section.

SHOWERHEAD FILM COOLED VANE COMPARISION

Film Cooled Thin Film Gauge Data Reduction

The thin film gauge, film cooled data reduction makes a distinction from the uncooled TFG data reduction in that instead of calculating recovery temperature from equation 6, it is measured during an uncooled run. Expanding equation 5 to include the total mainstream temperature results in

$$q_0" = h_0(T_{o,\infty} - T_w) - h_0(T_d) \tag{12}$$

where, T_d, is constant for constant Mach number. The equation is of the form y=mx+b, so h and T_r can be extracted from an experiment run with the coolant supply shut off using a linear regression technique. Figure 15 presents a sample of this technique.

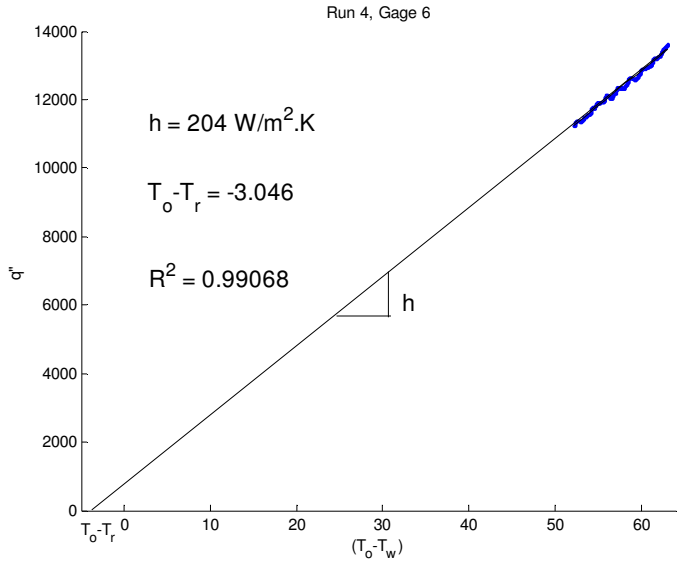

Figure 15. Example linear regression of Film Cooled Vane, BR = 0, TFG data

Film cooling effectiveness for the TFG data reduction is defined as:

$$\eta = \frac{T_{aw} - T_r}{T_c - T_r} \tag{13}$$

For film cooled cases equations 5 and 13 can be combined to yield:

$$\frac{q''}{T_r - T_c} = h\left(\frac{T_r - T_w}{T_r - T_c}\right) - h\eta \tag{14}$$

where T_c and T_w are measured during the experiment, q" is calculated with the finite difference code and T_r was measured during an uncooled experiment at the same gauge location. Equation 3 is in the form of y=mx+b which can be solved with a linear regression for h and η, a sample of which is shown in Figure 16. Previous thin film gauge experiments in the Virginia Tech Transonic Cascade [12, 13, 14, 15] have used this method to measure heat transfer coefficient, effectiveness, and recovery temperature. This data reduction technique is also outlined by Smith *et al.* [9].

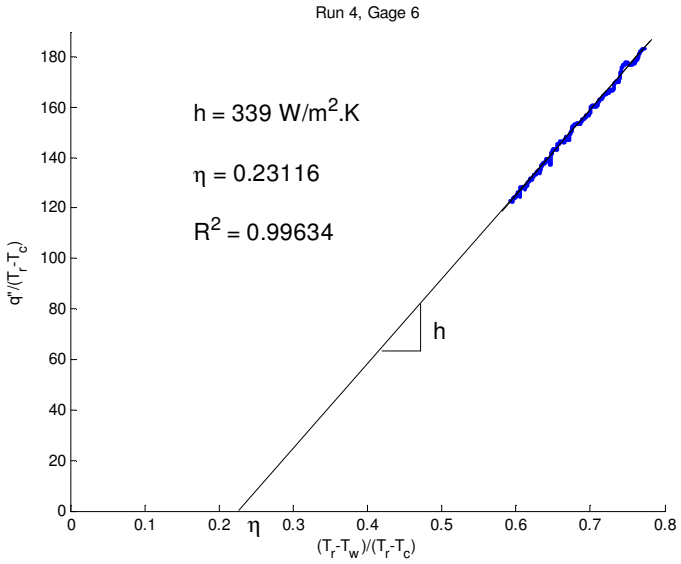

Figure 16. Example linear regression of Film Cooled Vane TFG Data, BR =2

Film Cooled Infrared Data Reduction Matlab Method

For film cooling situations, T_{aw} is replaced by film temperature, T_f, in equation 5. Film temperature is a function of the mainstream temperature, coolant temperature and mixing at the surface. Film cooling effectiveness is defined as:

$$\eta = \frac{T_f - T_\infty}{T_c - T_\infty} \tag{15}$$

the key difference being that mainstream temperature is used instead of local recovery temperature. Incorporating T_f into equation 10 results in the wall temperature equation:

$$\frac{T_w - T_i}{T_f - T_i} = 1 - \exp\left(\frac{h^2 \alpha t}{k^2}\right) erfc\left(\frac{h\sqrt{\alpha t}}{k}\right) \tag{16}$$

Vedula and Metzger [18] developed this technique for determination of h and η from a single transient test. With the previous uncooled results comparing well between the TFG and IR data sets, the Matlab program used for the uncooled case was adapted to add the additional parameter, T_f, which was then substituted for using the definition of η. Matlab was again employed to execute the fminsearch function to solve for the two parameters of interest, h and η. The measured wall temperature was plotted and the code attempted to curve fit h and η to match the wall temperature history using the equation:

$$T_{Fitted} = \left[\eta T_C + (1-\eta) T_M - T_i\right] * \left[1 - \exp\left(\frac{h^2 \alpha t}{k^2}\right) * erfc\left(\frac{h\sqrt{\alpha t}}{k}\right)\right] + T_i \tag{17}$$

to minimize error between measured T_w and calculated T_{Fitted}. This technique however, was not able to decouple h and η in a single test. Multiple combinations of the variables would produce near identical wall temperature histories. The equation was also developed assuming a step change in mainstream temperature, which is not consistent with the temperature response in the Virginia Tech Transonic Cascade. The code was

written to incorporate a changing mainstream temperature into the curve fitting function, however the unconstrained nonlinear optimization function, fminsearch, could not solve for a unique set of film cooling performance parameters without additional inputs leading this technique to be abandoned.

Film Cooled Infrared Data Reduction Fortran Method

The next method used to reduce the IR data is explained below. Equation 16, which was written for a step change in temperature, is again the starting point. To account for the transient mainstream temperature Duhamel's superposition theorem is used to simulate the mainstream temperature as a set of superposed steps:

$$T_w - T_i = \sum_{j=1}^{N} U(t-\tau_j)(T_f - T_i) \tag{18}$$

where:

$$U(t-\tau_j) = 1 - \exp\left(\frac{h^2\alpha(t-\tau_j)}{k^2}\right) erfc\left(\frac{h\sqrt{\alpha(t-\tau_j)}}{k}\right) \tag{19}$$

T_f is time varying and unknown in this equation but can be related through the definition of effectiveness, equation 15, where T_m is also time varying. Taking equation 18 at two separate time instances, the two equations can be iteratively solved for both h and η. Vedula and Metzger [18] never actually applied this method to simultaneously solve for both h and η with a single test, this was accomplished by Ekkad *et al.* [19] using the IR method. The IR results presented in this paper have been calculated using this method to solve for h and η with IR thermography.

Results

The results for the showerhead film cooled vane are presented in this section. Figure 17 provides a heat transfer coefficient plot for IR and TFG data while Figure 18

provides an effectiveness plot for IR and TFG data. The conclusion is that the IR and TFG data sets do not compare well. Heat transfer coefficient is higher across the entire vane surface for the TFG method and shows a different trend on the suction surface entirely. One positive is that the IR data does predict an earlier laminar to turbulent boundary layer transition compared to the BR=0 case which is seen in the TFG data as well. For the film cooling effectiveness plot, the pressure side trend compares favorably but there is a much faster decay downstream of injection. The suction surface effectiveness has the most glaring differences between the two methods. There is almost zero measured effectiveness directly downstream of injection using the IR technique while the TFG technique has results of approximately 0.30 at the first measurement location, followed by a reasonable decay further downstream. Further discrediting the comparison is a spike in effectiveness after X/C = 0.5 in the IR data that is not physically believable. The next few sections will attempt to analyze the possible causes for the differences in h and η values.

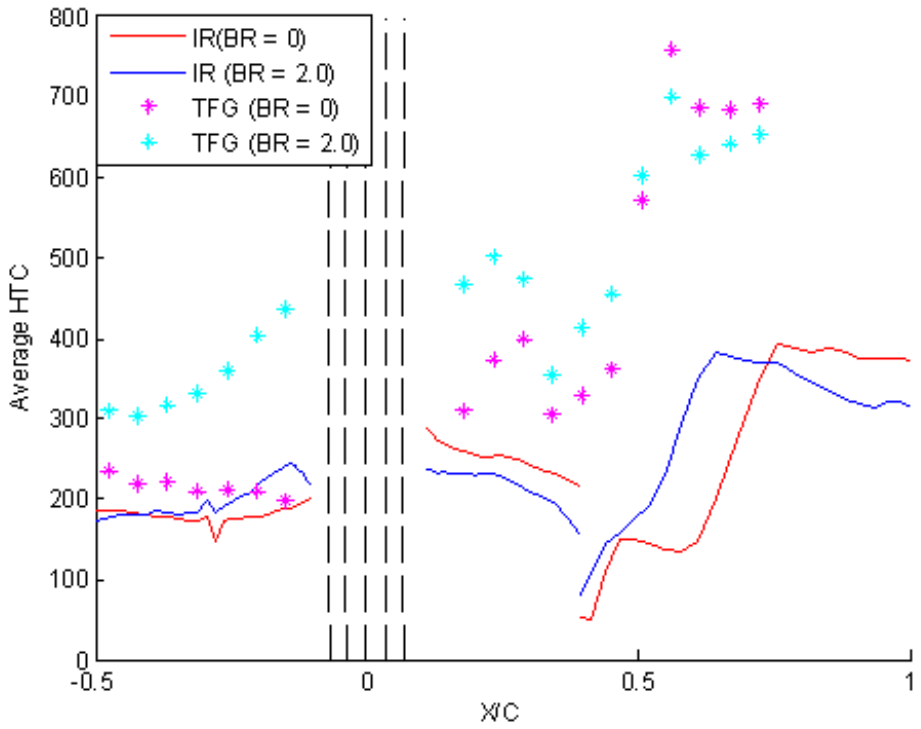

Figure 17. Showerhead Film Cooled Vane h, M_{ex} = 0.76, Tu = 16%

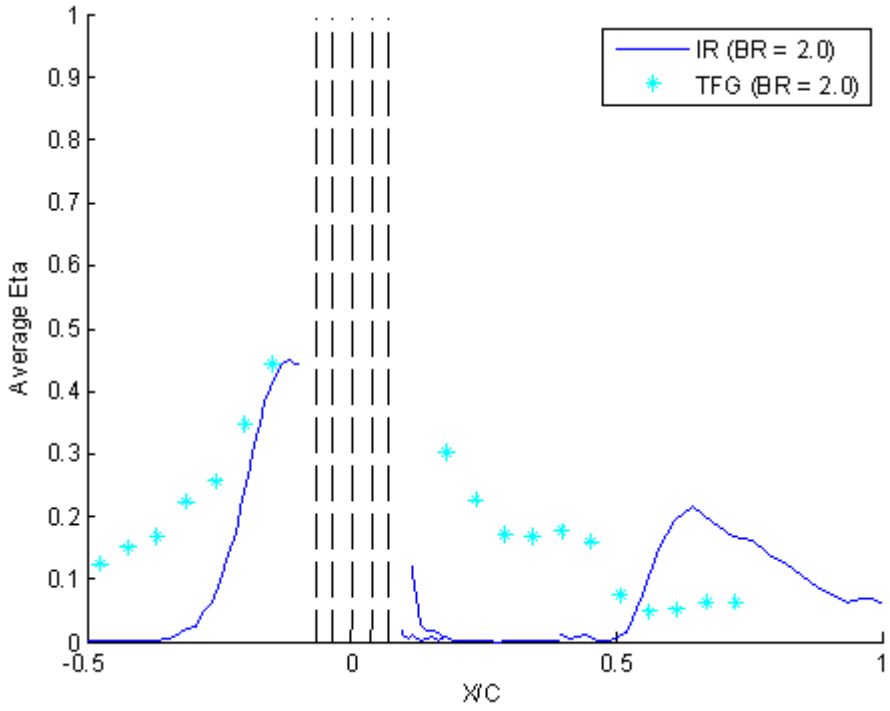

Figure 18. Showerhead Film Cooled Vane η, M_{ex} = 0.76, Tu = 16%

Analysis

Recovery Temperature Effect

The effect of recovery temperature is analyzed in this section. Recovery temperature is defined as the temperature of a moving fluid when brought to rest adiabatically. Total temperature by contrast is defined as the temperature of a moving fluid when brought to rest isentropically which is by definition, adiabatic. At higher speeds this provides a noticeable difference that should be accounted for. The typical method of calculating recovery temperature is using a relationship such as equation 6 relating recovery temperature, total temperature, and flow speed. This method was used in the TFG uncooled data reduction, for the TFG film cooled reduction, recovery temperature was measured, and finally for the IR data reduction recovery temperature was ignored. Figure 19 below shows a plot of T_d for measured recovery temperature and calculated (assuming a recovery factor for turbulent boundary layers) values. Based on the definition of recovery temperature, it is not physical to measure recovery

temperatures that are hotter than the total temperature (negative T_d values). While the theory behind measuring recovery temperature is sound, the negative values and excessive positive values may be due to errors in the measurement or data reduction technique. The sensitivity to these three applications of recovery temperature is discussed below.

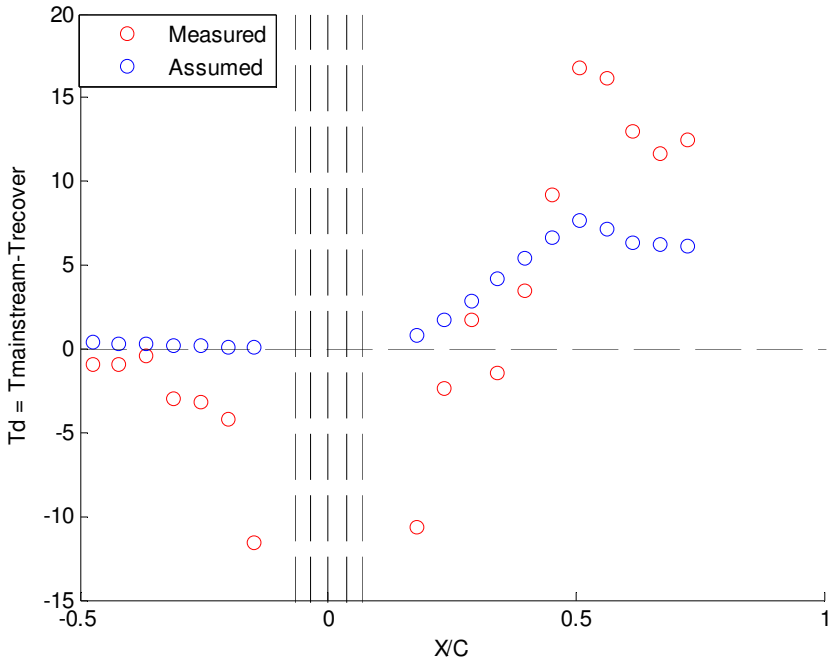

Figure 19. Measured and Assumed Recovery Temperatures

The application of recovery temperature was analyzed as a possible explanation for the discrepancies between the TFG and IR techniques. Due to the difficulties in finding surface locations in the IR data, the TFG data is used here for analysis. Figure 20 plots the effects of ignoring recovery temperature (IR reduction), calculating recovery temperature and measuring recovery temperature (TFG reduction) on heat transfer coefficient. From this figure, negative T_d values increase heat transfer coefficient, while positive T_d values decrease heat transfer coefficient. However, recovery temperature does not significantly affect the h trend. However this is not the case for η as shown in Figure 21. Recovery temperature has a first order effect and causes a decreasing trend for effectiveness on the suction side when the ignored and calculated T_d trends are still

increasing. It is interesting to note that this increasing trend far downstream of injection is seen in the IR results where recovery temperature is also ignored. Negative values of T_d cause direct increases in η while positive values decrease η. Incorporating calculated recovery temperature into the IR reduction technique will reduce the spike far downstream of injection seen in Figure 18, however it will not increase η from zero directly downstream of injection.

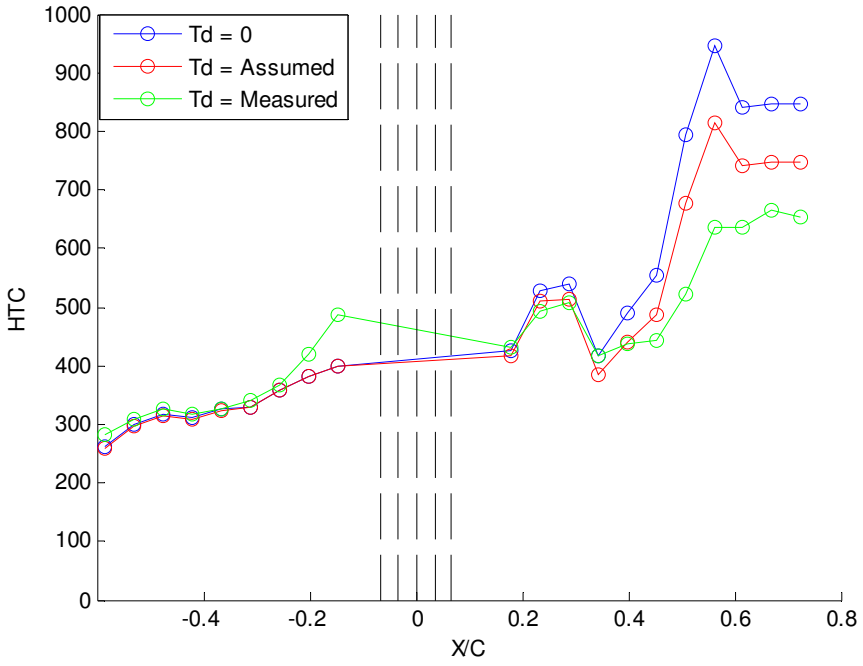

Figure 20. Effect of T_d on h for TFG data reduction

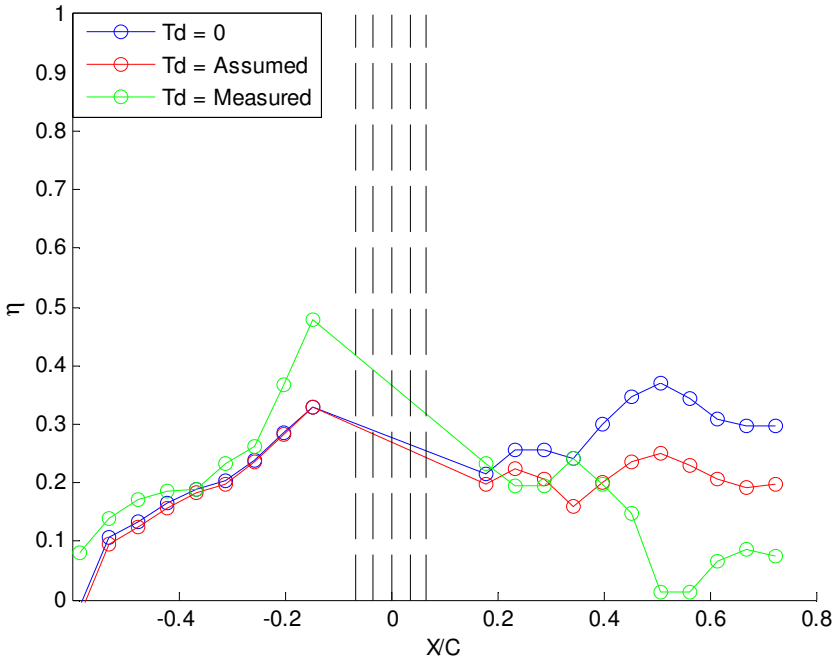

Figure 21. Effect of T_d on η for TFG data reduction

Data Reduction Analysis

This section will present results using the raw temperature data in different reduction programs. To check that the discrepancies were not being caused by the data reduction programs, a thorough analysis of both programs were done to eliminate the code as a source of error. Figures 22 and 23 present h and η results from the TFG raw temperature data. The original results from the TFG reduction are included as well as the results where the recovery temperature effect is ignored for comparison since the Fortran program also ignores recovery temperature. Also, the Fortran program did not account for a composite heat transfer surface, TFG wrapped around Macor, so results for both material properties were included. The h results follow the same trend and are enveloped by the Fortran programs predicted results for Macor and Kapton properties. The η results are more intriguing in that there is little effect of the material properties on the values, the trend is still similar, and the values are predicted higher at all points by the Fortran program.

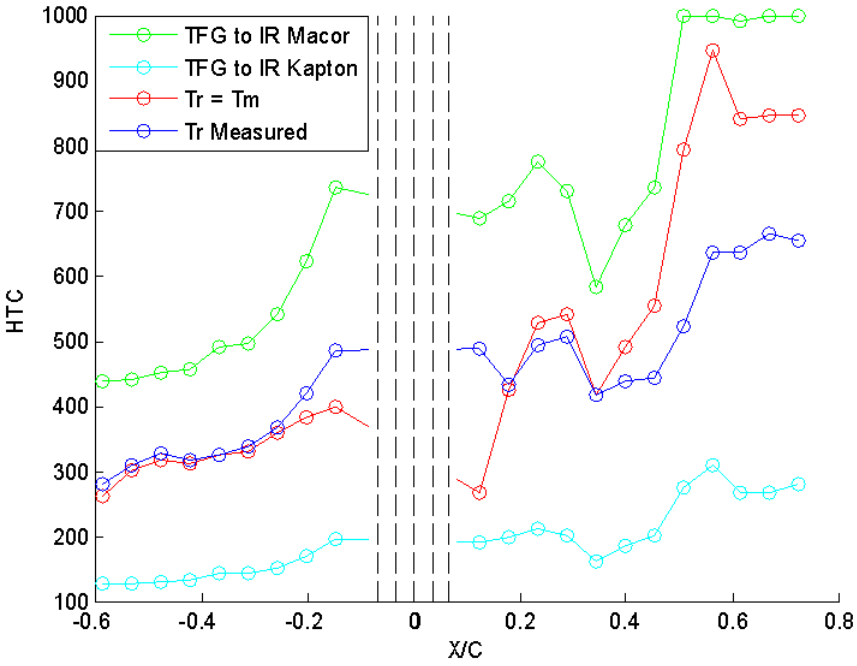

Figure 22. TFG data *h* comparison between TFG and Fortran IR Reduction.

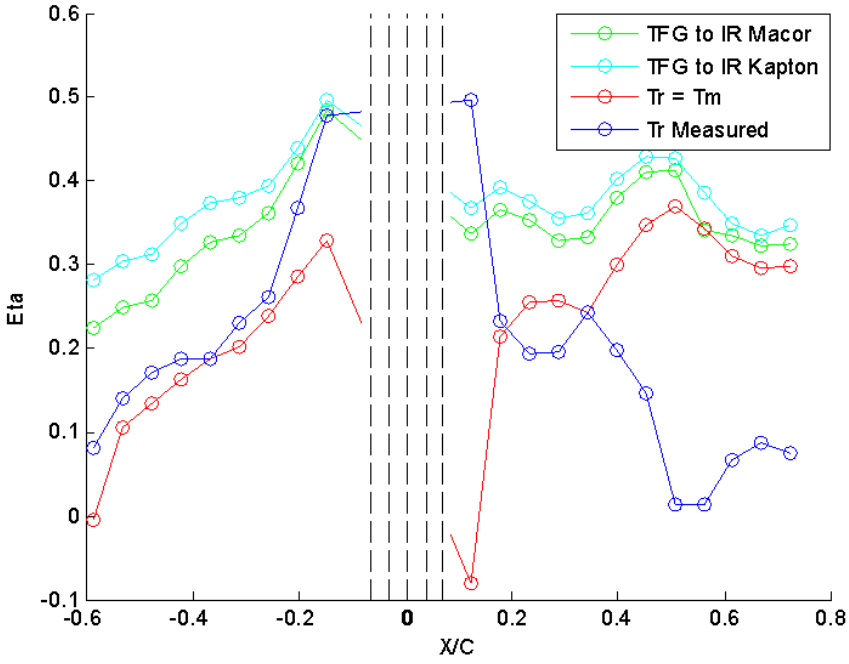

Figure 23. TFG data η comparison between TFG and Fortran IR Reduction.

Now the reverse procedure is also executed with the IR data. It should be noted that IR data did not work as nicely with the finite difference code calculation of heat flux

as the TFG data did. The *q"* was noticeably noisy and did not follow a smooth curve. This resulted in significant noise in the linear regression procedure and low R^2 values characterizing the line fit. A sample is presented in Figure 24. This did not diminish the effect of the exercise though as discussed below.

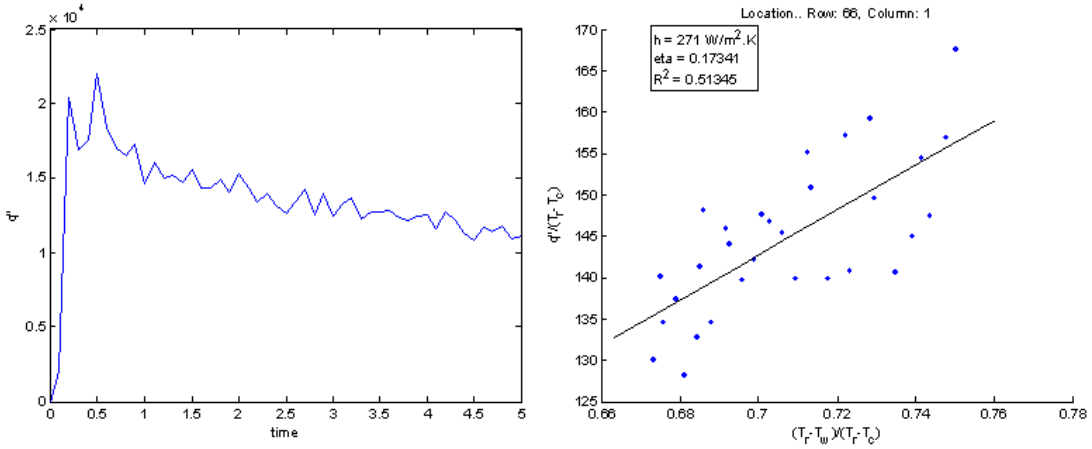

Figure 24. Sample q" calcuation and resulting linear regression.

Figures 25 and 26 presents a comparison of the *h* and *η* results that were calculated using the IR temperature data with the IR reduction method and the TFG reduction method. Results are presented for two window views, PS and SS. The *h* trend and values are very similar between the two techniques. However, There is a noticeably higher *h* on the suction surface downstream of X/C = 0.6. This was also noticed in the uncooled comparison. Both results use the same finite difference code to calculate *q"*, which may be predicting higher heat flux in this region of the vane. This may be affecting the *η* levels in the same region even though similar *η* trends are calculated using both data reduction techniques. There are some spikes on the pressure surface downstream of X/C = -0.2 that can be attributed to poor R^2 values and the resulting extrapolation errors.

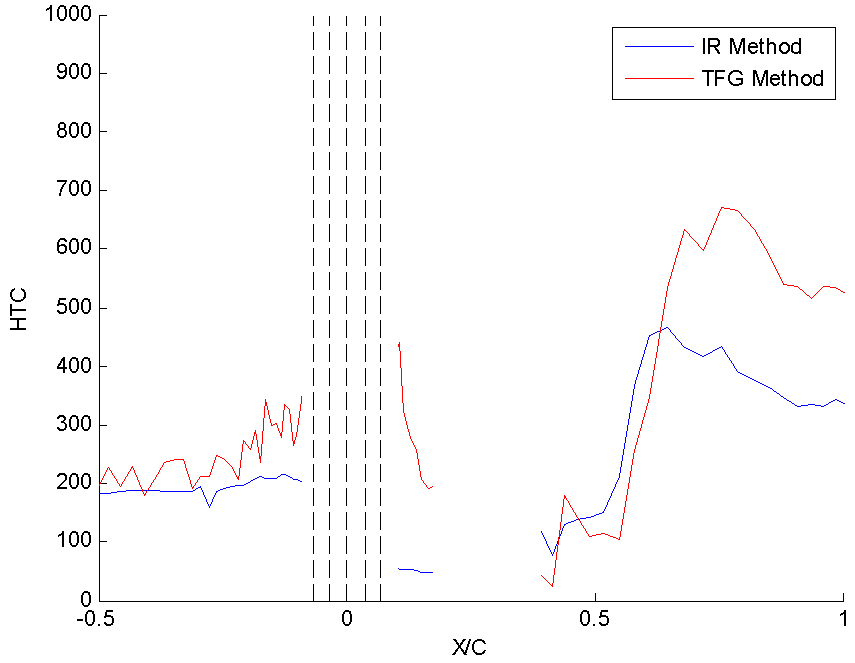

Figure 25. IR data *h* comparison between TFG and Fortran IR Reduction

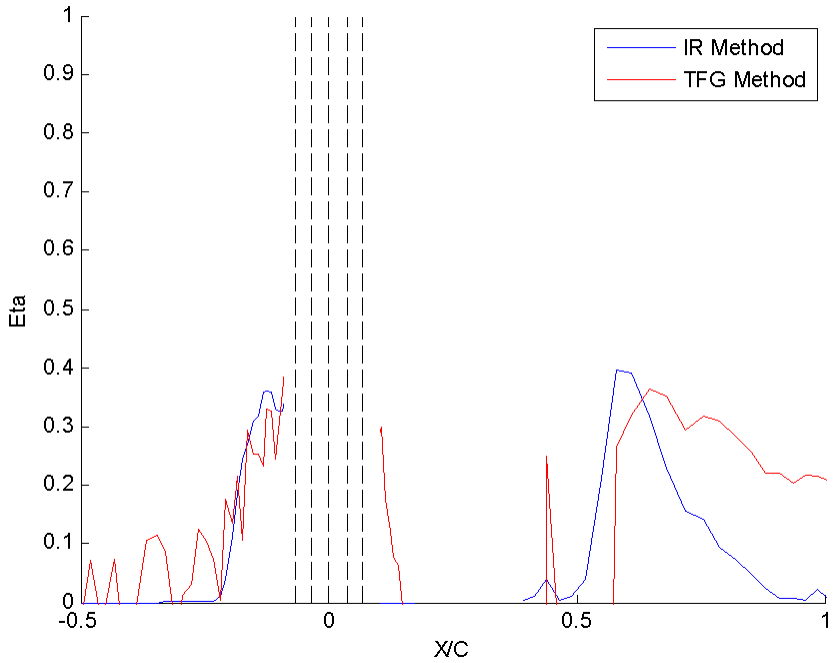

Figure 26. IR data η comparison between TFG and Fortran IR Reduction.

The conclusion, however, is that the difference in data reduction program execution cannot account for the difference in trend or values seen between the IR and TFG data sets. However, the exercise presented here has produced some novel ideas on how to account for recovery temperature in the IR program that will be explored and executed in the future.

Possible Reflected Radiation Effects

Having exhausted the analysis of the data reduction programs without a resolution to the IR effectiveness trend, a physical analysis of the experiment was revisited. In the experiment preparation, the cascaded hardware was spray painted black to increase the emissivity of the surface. The sidewalls and windows were also sprayed to minimize reflections in the surface. However, an oversight was made with the adjacent, pressure tapped vanes. The midspan of the vane was covered with a ¾in strip of tape during the painting process so the pressure taps would not clog. The strip of aluminum shown in Figure 27a was presumed harmless until after all the data had been taken, reduced, and extensively analyzed without successfully validating the IR technique.

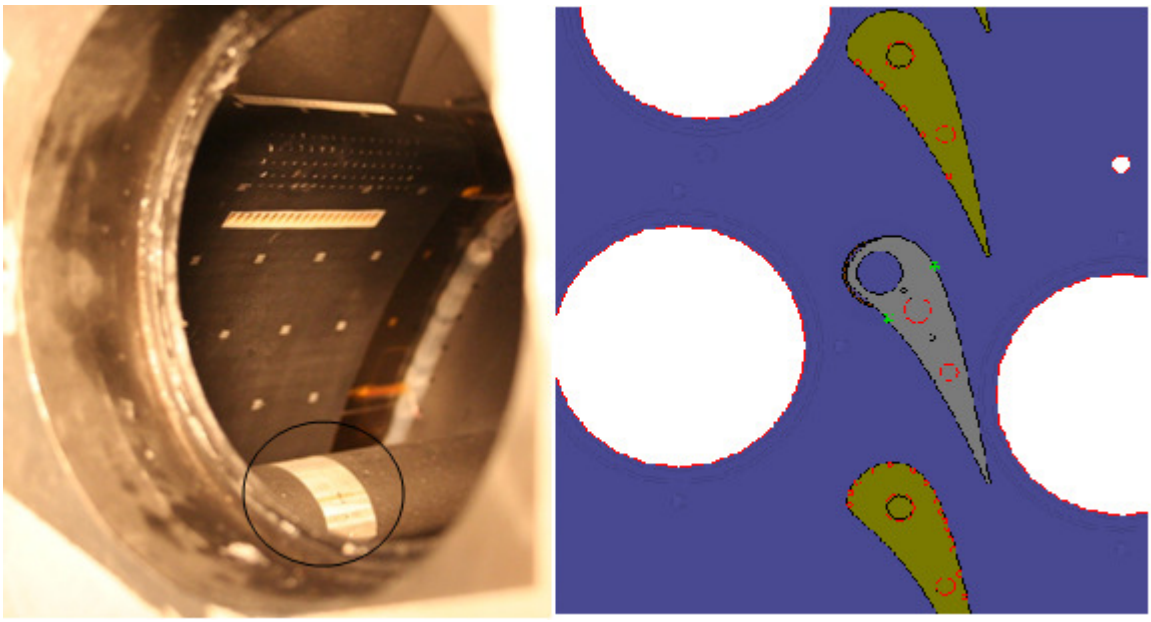

(a) **(b)**

Figure 27. (a) Al strip (b) Cascade geometry w pressure taps (red circles).

Reflected radiation is a complex problem involving temperature gradients, surface properties, view factors, and shape factors and in the end, it may prove to be a non-issue. However, the IR reduction is incredibly sensitive to changes in the wall temperature curve. A 1.2 C^o reduction at 2s and a 2.7 C^o reduction at 5s were tested at a single pixel to simulate a possible measurement error due to reflected radiation in a transient temperature environment. The initial wall temperature history as measured resulted in an h=225 and η=0. Using the simulated measurement error described above, h=389 and η=0.38. If the surfaces adjacent to the pressure taps shown in Figure 27b reflect radiation and artificially increases the measured wall temperature, it could explain the region of zero effectiveness downstream of injection and subsequent bump after X/C=0.5 and possibly the pressure side effectiveness decay. The effect of reflected radiation is only a theory at this point but is worthy of further investigation by painting these surfaces and retesting.

SHAPED HOLE VANE

Blowing Ratio Conditions

This section will present the blowing ratios at each injection location. The initial motivation of this experiment was to test the effect of blowing ratio on combined showerhead and shaped hole injection at 3 different Mach numbers. Due to the difficulties described in validating the IR technique, only one Mach number, 0.85 was tested. The local blowing ratios for each injection location are presented in Table 4. The method for calculating blowing ratio was described in the Film Cooling Supply section.

Table 4. Blowing Ratio for each injection location

	Blowing Ratio Calculations		
Showerhead	1.7	2.0	2.8
Suction	1.3	1.5	1.8
Pressure	4	5	6.5

Results

This section will present the showerhead and shaped hole film cooled vane results for comparison. Although three blowing ratios are presented, the BR=2.0 case is the most interesting since it compares similar flow conditions to the showerhead film cooled vane presented earlier, also measured with IR. Figures 28 and 29 present the h and η results for all blowing ratios. Film cooling injection augments heat transfer coefficient and causes an earlier laminar to turbulent boundary layer transition on the suction surface as also seen on the showerhead film cooled vane. The pressure surface effectiveness trend decays quickly downstream of the pressure side shaped hole. The suction surface effectiveness trend exhibits the same rapid decay directly downstream of injection as seen on the showerhead film cooled vane and also the large bump in effectiveness after X/C=0.5. This trend is intriguing in that both results for shaped hole vane and the showerhead film cooled vane are unrealistic but consistent. This is cause for further investigation and testing with the film cooled IR measurement technique.

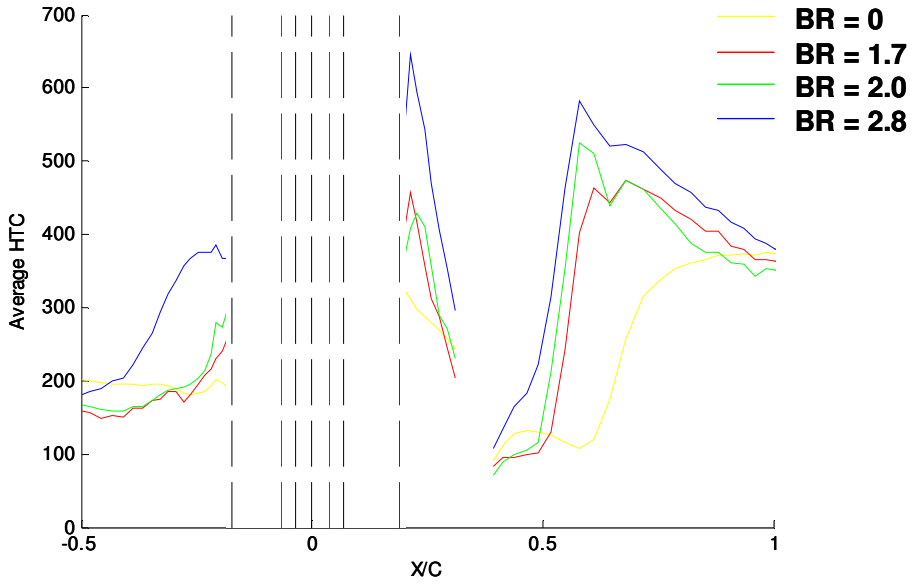

Figure 28. Shaped Hole Vane h, M_{ex} = 0.85, Tu = 13%

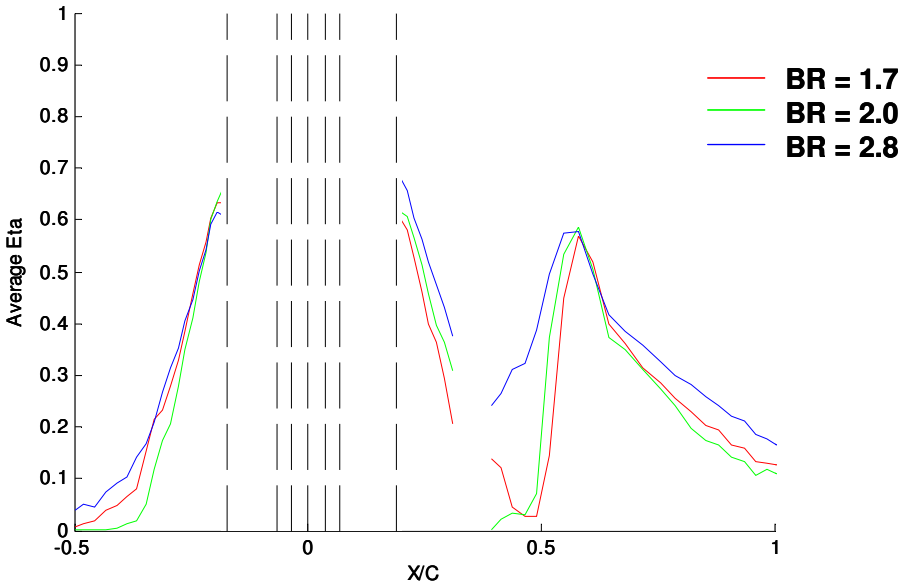

Figure 29. Shaped Hole Vane η, M_{ex} = 0.85, *Tu* = 13%,

CONCLUSIONS

This thesis presents a comparison of two surface temperature measurement techniques, TFG and IR, at transonic conditions. Two comparisons were made with thin film gauge results. A relatively good comparison was made for the uncooled vane between IR and TFG, however room for improvement was identified. The showerhead film cooled vane comparison was not as successful. Glaring differences between the results produced by the two measurement techniques were found. Analysis of the techniques identified and quantified differences caused by the reduction methods and noted one possible source of error in the measurement caused by an oversight in experiment preparation. Results for a showerhead and shaped hole cooled vane were presented as a second film cooling geometry measured with IR. Comparable showerhead blowing ratios were used for one of the shaped hole vane cases which showed similar, but unrealistic, suction side trends. Drastic steps forward have been made in establishing a reliable and robust method of determining heat transfer coefficient and film cooling effectiveness at transonic conditions using infrared thermography. However, there are still questions that must be answered and improvements that must be made to complete the development of this technique.

REFERENCES

[1] Han, J., Dutta, S., and Ekkad, S., 2000, *Gas Turbine Heat Transfer and Cooling Technology*, Taylor & Francis, New York.

[2] Bogard, D.G., and Thole, K.A., 2006, "Gas Turbine Film Cooling," *ASME J. Propulsion and Power,* 22, pp. 249-270.

[3] Bunker, R.S., 2005, "A Review of Shaped Hole Turbine Film-Cooling Technology," *ASME J. of Heat Transfer,* 127, pp 441-453.

[4] Abuaf, N., Bunker, R., and Lee, C.P., 1997, "Heat Transfer and Film Cooling Effectiveness in a Linear Airfoil Cascade," *ASME J. Turbomach.*, 119, pp. 302-309.

[5] Guo, S.M., Lai, C.C., Jones, T.V., Oldfield, M.L.G., Lock, G.D., and Rawlinson, A.J., 1998, "The Application of Thin-film Technology to Measure Turbine-Vane Heat Transfer and Effectiveness in a Film-Cooled, Engine-Simulated Environment," *Intl. J. Heat and Fluid Flow*, 19, pp. 594-600.

[6] Reiss, H., Bolcs, A., 2000, "The Influence of the Boundary Layer State and Reynolds Number on Film Cooling and Heat Transfer on a Cooled Nozzle Guide Vane," ASME 2000-GT-205

[7] Zhang, L., Moon, H.K., 2008 "The Effect of Wall Thickness On Nozzle Suction Side Film Cooling," ASME GT 2008-50631.

[8] Ekkad, S.V., Ou, Shichuan, Rivir, R.B., 2004, "A Transient Infrared Thermography Method for Simultaneous Film Cooling Effectiveness and Heat Transfer Coefficient Measurements From a Single Test," *ASME J. Turbomach.*, 126, pp. 597-603.

[9] Smith, D.E., Bubb, J.V., Popp, O., Grabowski, H.C., Diller, T.E. Schetz, J.A. and Ng. W.F., 2000, "An Investigation of Heat Transfer in a Film Cooled Transonic Turbine Cascade, Part I: Steady Heat Transfer," ASME GT-2000-202.

[10] Popp, O., Smith, D.E., Bubb, J.V., Grabowski, H.C., Diller, T.E. Schetz, J.A. and Ng. W.F., 2000, "An Investigation of Heat Transfer in a Film Cooled Transonic Turbine Cascade, Part II: Unsteady Heat Transfer," ASME GT-2000-203.

[11] Nix, A.C., Diller, T.E., and Ng, W.F., 2007, "Experimental Measurements and Modeling of the Effects of Large-Scale Freestream Turbulence on Heat Transfer," *ASME J. Turbomach.*, 129, pp. 542-550.

[12] Carullo, J.S., Nasir, S., Cress, R.D., Ng, W.F., Thole, K.A., Zhang, L.J, and Moon, H.K., 2007, "The Effects of Freestream Turbulence, Turbulence Length Scale, and Exit Reynolds Number on Turbine Blade Heat Transfer in a Transonic Cascade," ASME GT-2007-27859.

[13] Nasir, S., Carullo, J.S., Ng, W.F., Thole, K.A., Wu, H., Zhang, L.J., and Moon, H.K., 2007, "Effects of Large Scale High Freestream Turbulence, and Exit Reynolds Number on Turbine Vane Heat Transfer in a Transonic Cascade," ASME IMECE-2007-44098.

[14] Nasir,S., Bolchoz, T., Ng, W.F., Zhang, L.J., Moon, H.K., and Anthony, R.J., 2008, "Showerhead Film Cooling Performance of a Turbine Vane in a Transonic Cascade," ASME IMECE-2008-66528.

[15] Bolchoz, T., Nasir, S., Reagle, C., Ng, W.F., and Moon, H.K., 2009, "An Experimental Investigation of Showerhead Film Cooling Performance In A Transonic Vane Cascade At Low and High Freestream Turbulence," GT2009-59796.

[16] Gritsch, M., Schulz, A., and Wittig, S., 1998, "Discharge Coefficient Measurements of Film-Cooling Holes With Expanded Exits," *J. of Turbomach.*, 120, pp. 557-563.

[17] Carslaw, H.S., and Jaeger, J.C., 1959, *Conduction of Heat in Solids*, 2nd ed. Oxford University Press, London.

[18] Metzger, D.E., and Larson, D.E., 1986, "Use of Melting Point Surface Coatings for Local Convective Heat Transfer Measurements in Rectangular Channel Flows with 90-Deg Turns," *ASME J. Heat Transfer*, 108, pp.48-54.

APPENDIX

VANE AERODYNAMIC MEASUREMENTS

The surface Mach number distribution is supplied in Figure A for the uncooled vane at Exit Mach 0.8. These aerodynamic measurements were performed by Nasir *et al.* [13] and were used to calculate recovery temperature using equation 6. The flow rapidly accelerates on the suction side up to the throat at s/C = 0.51, after which it decelerates to the trailing edge. The pressure side continuously accelerates from the leading edge to trailing edge. Figure B plots the corresponding acceleration parameter, K, for the smooth, uncooled vane. Mayle [19] noted the critical value of K to be 3×10^{-6}. Acceleration parameter values above this criteria prevent laminar to turbulent transitions and can relaminarize turbulent boundary layers.

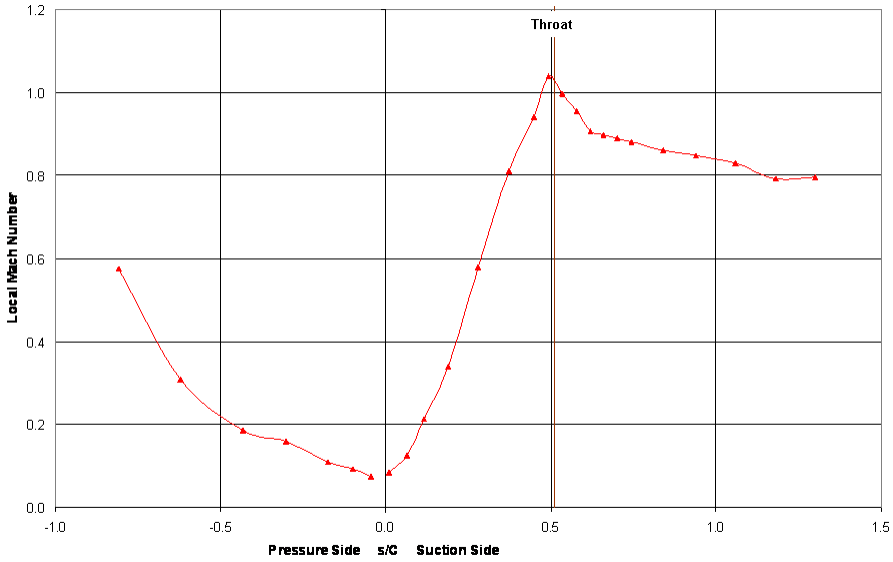

Figure A. Vane Mach Number Distribution

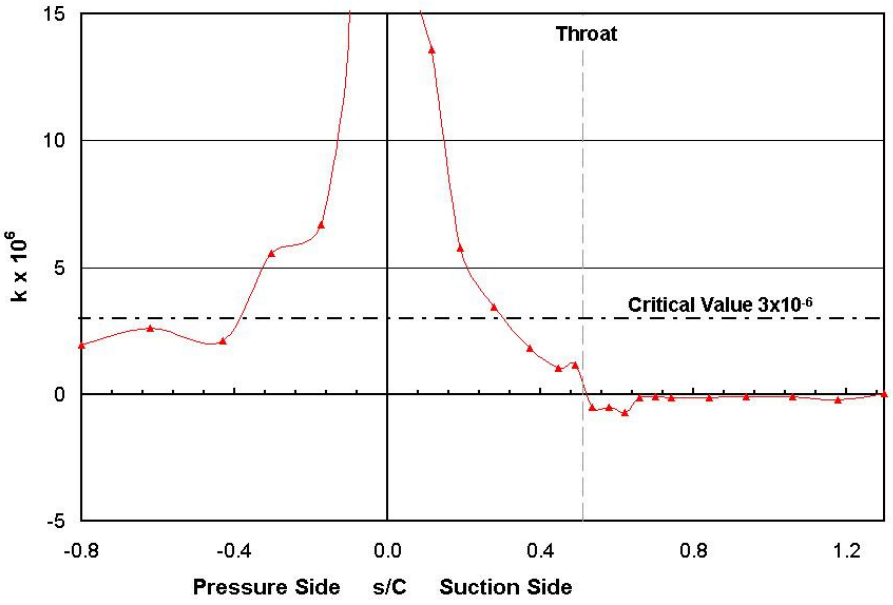

Figure B. Vane Acceleration Parameter

[19] Mayle, R.E., 1991, "The Role of Laminar-Turbulent Transition in Gas Turbine Engines," *ASME J. of Turbomach.,* 113, p. 509-537.